JOURNAL OF VIROLOGY, Sept. 2002, p. 8842–8854 Vol. 76, No. 17
0022-538X/02/$04.00+0 DOI: 10.1128/JVI.76.17.8842–8854.2002

Enhanced Cytomegalovirus Infection of Developing Brain Independent of the Adaptive Immune System

Anthony N. van den Pol,[1]* Jon D. Reuter,[2] and Justin G. Santarelli[1]

Departments of Neurosurgery[1] and Comparative Medicine,[2] Yale University School of Medicine, New Haven, Connecticut 06520

Received 26 March 2002/Accepted 31 May 2002

Cytomegalovirus (CMV) has been suggested as the most prevalent infectious agent causing neurological dysfunction in the developing brain; in contrast, CMV infections are rare in the adult brain. One explanation generally given for the developmental susceptibility to the virus is that the developing immune system is too immature to protect the central nervous system from viral infection, but as the immune system develops it can protect the brain. We suggest an alternate view: that developing brain cells are inherently more susceptible to CMV infection, independent of the immune system. We used a recombinant mouse CMV that leads to green fluorescent protein expression in infected cells. Control experiments demonstrated a high correlation between the number of cells detected with the viral GFP reporter gene and with immunocytochemical detection of the virus. After intracerebral inoculation, the number of CMV-infected cells in neonatal brains was many times greater than in mature control or mature immunodepressed SCID mice, and the mortality rate of neonates was substantially greater than SCID or control adults. Parallel experiments with live brain slices inoculated in vitro, done in the absence of the systemic immune system, generated similar data, with immature hippocampus, hypothalamus, cortex, striatum, and cerebellum showing substantially greater numbers of infected cells (100-fold) than found in adult slices in these same regions. Interestingly, in the cerebellar cortex, CMV-infected cells were more prevalent in the postmitotic Purkinje cell layer than in the mitotic granule cell layer, suggesting a selective infection of some cell types not dependent on cell division. Together, these data support the view that CMV has an intrinsic preference for infection of developing brain cells, independent, but not mutually exclusive, of the developmental status of the systemic immune system in controlling CMV infection.

Cytomegalovirus (CMV) has been suggested as the leading viral cause of birth defects and neurological dysfunction (3, 47). Infections of the developing brain can lead to a number of problems, including mental retardation, epilepsy, microencephaly, microgyria, hydrocephalus, and deafness (4, 20, 33). The incidence of CMV-induced neurological problems has been estimated at 0.1% of births, with a possibility of more-subtle problems, such as learning deficits, in infected children (20, 23). In contrast to the susceptibility of the developing central nervous system (CNS), CMV is not a particular threat to the mature brain, except under conditions of a compromised immune system (21, 30).

CMV causes a number of cellular problems, including cytomegaly and syncytium formation, leading to cell death or viral latency. CMV shows substantial species specificity, replicating selectively in the host species. Mouse and human CMV each have genomes of 235 kb of double-stranded DNA, have similar tissue affinity, similar viral morphology and biology, similar ability to achieve long-term latency, and colinear gene sequences with different nucleotide sequences within many genes (22, 31, 30, 41). The majority of adult humans and wild mice have been infected by CMV (30, 31). Together, these factors suggest that the actions of mouse CMV may parallel its human counterpart.

A prevalent view is that CMV is more damaging to the developing brain than to the mature brain because the systemic immune system is too immature during development to fight CMV infection (7–10, 37). T- and antibody-generating B-lymphocytes of the adaptive immune system, as well as other cells of the systemic immune system, including natural killer cells and macrophages/monocytes, have been shown to combat CMV infections (3, 5, 18, 39) and the efficacy of these systems increases with development. However, an additional possibility that has not been directly tested is that the virus may have an intrinsic affinity for developing brain cells. This would be consistent with a relatively high level of reporter gene expression under control of the CMV IE1 promoter in the developing brains, but not mature brains, of transgenic mice (46). To test the hypothesis that CMV has a preference for infecting immature postnatal brain cells over mature brain cells, independent of immune status, we compared developing and adult mice of the same strain that were either immunocompetent or immunodeficient (SCID mice); SCID mice have deficiencies in both humoral and cellular immunity. To further address the same question, we did parallel corroborating experiments with CMV infection of live brain slices harvested from mice of different developmental ages and inoculated in vitro to eliminate the adaptive immune system as a factor in infection levels.

MATERIALS AND METHODS

Brain slices. Neonatal mice were anesthetized by hypothermia, and older mice were anesthetized with sodium pentobarbital (150 mg/kg). The brains were removed and then sliced into coronal sections several millimeters thick. These were then cut with a vibratome to a thickness of 200 um. Whole-brain slices were placed at the fluid-gas interface on a Millipore membrane with a 0.4-μm pore

* Corresponding author. Mailing address: Department of Neurosurgery, Yale University School of Medicine, 333 Cedar St., New Haven, CT 06520. Phone: (203) 785-5823. Fax: (203) 737-2159. E-mail: anthony.vandenpol@yale.edu.

size and fed with defined Neurobasal Medium (Gibco). Serum, which can stimulate the proliferation of dividing cells, was not used. Living brain slices were infected by adding medium containing 5×10^4 PFU of recombinant murine CMV (mCMV) to the slice. Slices were maintained at 37°C in a 5% CO_2 incubator.

Quantification of infected cells from in vitro slices. At 48 h after inoculation, brain slices were fixed by immersion in 4% paraformaldehyde. Cells infected with CMV were fluorescent due to the expression of the green fluorescent protein (GFP) reporter. The number of infected cells was counted by using a 400-μm square on each edge through a SZX12 Olympus fluorescent microscope and a GFP filter cube. All fluorescent cells within the test square were counted. A total of three to four slices from three mice of the same age were used, and 8 to 10 test squares were used for each of the eight brain regions studied. This allowed us to generate a mean (± the standard error of the mean [SEM]) number of infected cells for each area. Calcium digital imaging with the calcium-sensitive dye fluo-3 was used to demonstrate that cells in mature brain slices were alive. Recordings were made with an Axon digital imaging system (Axon Instruments) by using an excitation of 488 nm and an emission of 530 nm. A shutter blocked the fluorescent light between data captures. In time-lapse recordings, one image was saved every 4 s. During recording, slices were maintained in a HEPES buffer (44). After we recorded a control baseline fluorescence, the cells were stimulated with a micropipette as described elsewhere (12). To affirm that CMV was replicating in slices, some slices were incubated in bromodeoxyuridine (BrdU) and, at 48 after inoculation, slices were fixed in 4% paraformaldehyde. BrdU was detected with a rat monoclonal antibody (Accurate) against BrdU (1:1,000 in phosphate-buffered saline with 0.3% Triton X-100) and then labeled with a goat anti-rat secondary antiserum conjugated to Texas red (1:250; Molecular Probes).

mCMV. Recombinant mCMV (gift of J. Vieira) was used that had an enhanced GFP with codons corrected for the mammalian sequence. This was driven by an elongation factor 1a promoter, placed at the IE2 site, a site that did not alter viral replication or tissue preference (11), as previously described (42). Green fluorescence could be found in infected brain cells within 6 h of CMV inoculation (42).

Immunocytochemistry. A monoclonal antibody (a gift of J. Nelson) against mCMV IE1, diluted 1:1,000 in phosphate-buffered saline with 0.3% Triton X-100, was used to reveal cells infected with mCMV and to compare them with the GFP reporter. A secondary antibody of goat anti-mouse immunoglobulin conjugated to Texas red (Molecular Probes) was used at 1:200 to localize immunoreactive cells. Controls included the omission of the primary antiserum and the use of noninoculated tissue where no immunostaining was expected or found.

Digital and confocal laser imaging. Photomicrographs were made with a Spot 2 digital camera (Diagnostic Instruments) interfaced with a Macintosh computer. Contrast was corrected in Photoshop, and images were printed on an Epson 870 digital printer. Some images were taken with an Olympus Fluoview 300 Confocal Scanning Microscope. An argon ion laser was used to detect GFP, and a helium-neon laser was used to detect Texas red in the same tissue section.

In vivo experiments. We used SCID mice (Harlan) that have a depressed immune system. SCID mice have a genetic deficit in DNA repair, resulting in a dramatic reduction in the number of both B and T cells (16, 19). Controls were of the BALB/c strain, the same strain from which the SCID mice were derived. Intracerebral injections were made into the brain of anesthetized mice (hypothermia anesthesia for neonates; 100 mg of ketamine and 10 mg of xylazine/kg for adults). For neonatal mice, a glass pipette with a tip diameter of 100 μm was fashioned on a micropipette puller (Narashige) and connected to a 1-μl Hamilton microsyringe. Injections of 500 nl (2.5×10^5 or 2.5×10^4 PFU) were given into the left cortex at postnatal day 1. Adult SCID and control mice (all 35 days old) were inoculated with mCMV by using a Hamilton microsyringe through a small hole in the skull with 1 μl (i.e., the same number of PFU as for the neonates) of mCMV. After inoculation, mice were kept warm in their home cage until they were mobile. Since subsequent analysis showed a substantial overlap in the number of infected cells in mice receiving the two doses and since no statistical difference was found between the groups receiving the two concentrations, the groups were combined. Some infected neonatal mice became dehydrated and moribund, stopped nursing, showed signs of motor dysfunction, and showed no sign of recovery; these mice were killed with 100% carbon dioxide gas before the 6-day postinoculation endpoint and were considered to have shown a lethal response to the virus.

At 6 days after inoculation, mice were killed with an overdose of 100% carbon dioxide and immediately perfused transcardially with physiological saline containing heparin, followed by 4% paraformaldehyde. After cryoprotection in 15% and then 30% sucrose, 15-μm-thick sections were cut through the entire brain, and 1 of every 30 neonate sections or 1 of every 60 adult sections was used for analysis after being mounted on glass slides. The total number of infected cells was estimated by multiplying the mean number of cells counted per section by the total number of sections (i.e., multiplication by 30 for neonates and multiplication by 60 for adults). Sections were evaluated on an Olympus IX70 inverted microscope or an SZX12 upright microscope by using standard enhanced GFP excitation and emission filters (Filter 41001; Chroma, Brattleboro, Vt.). All quantitation of the infected cell numbers was done with the SZX12 microscope. Animal use for this series of experiments was approved by the Yale University Animal Care and Use Committee.

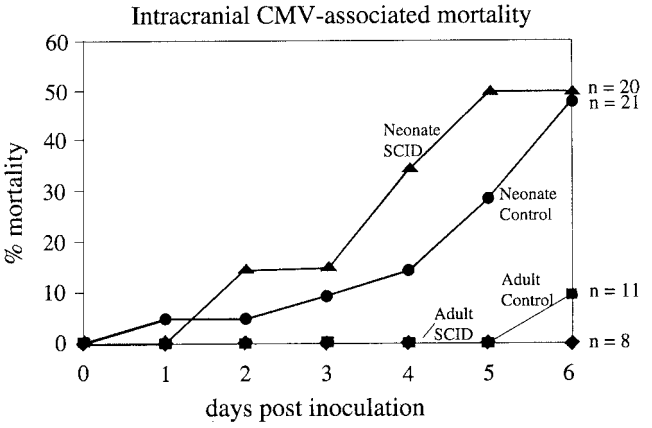

FIG. 1. Survival after CMV infection in adult and neonatal SCID and control mice. This graph plots the survival of the four groups of mice after CMV inoculation. Mortality was highest for both neonate groups (thick lines) compared with adults (thin lines). The number of mice per group at the beginning of the experiment is shown on the right.

RESULTS

The results are divided into two sets of experiments. The first set focuses on the relative contribution of age and immune status to virus infection after intracerebral inoculation of CMV in neonatal and adult immunocompromised and control mice. The second set of experiments employs live brain slices in vitro to assess the influence of the developmental stage on CMV infection in the absence of the adaptive immune system.

Intracerebral administration of CMV. Adult SCID and control mice received intracerebral injections of mCMV and 6 days later were given an overdose of anesthetic and perfused with fixative for histological analysis. In contrast to the control and SCID adults that continued to appear healthy after intracerebral inoculation, when neonatal mice were infected intracerebrally with CMV the health of the neonates showed substantial deterioration. Whereas only 1 of 19 (5%) adults (out of 8 SCID mice and 11 controls) died in the course of the experiments, a high percentage of neonatal mice died (49% [20 of 41]) out of 20 SCID and 21 control mice (Fig. 1). The mortality rate was equally distributed between neonatal SCID and neonatal control groups (Fig. 1).

Histological sections were cut from the brains of infected and noninfected control mice. No fluorescent cells were found in noninfected control sections. In contrast, in CMV-inoculated brains, infected cells could be detected by the bright fluorescence generated by the GFP reporter. Differences in the number of cells infected were strikingly apparent between the mildly infected adult SCID (Fig. 2A) and heavily infected neonate SCID (Fig. 2B). Although in the cell counts described

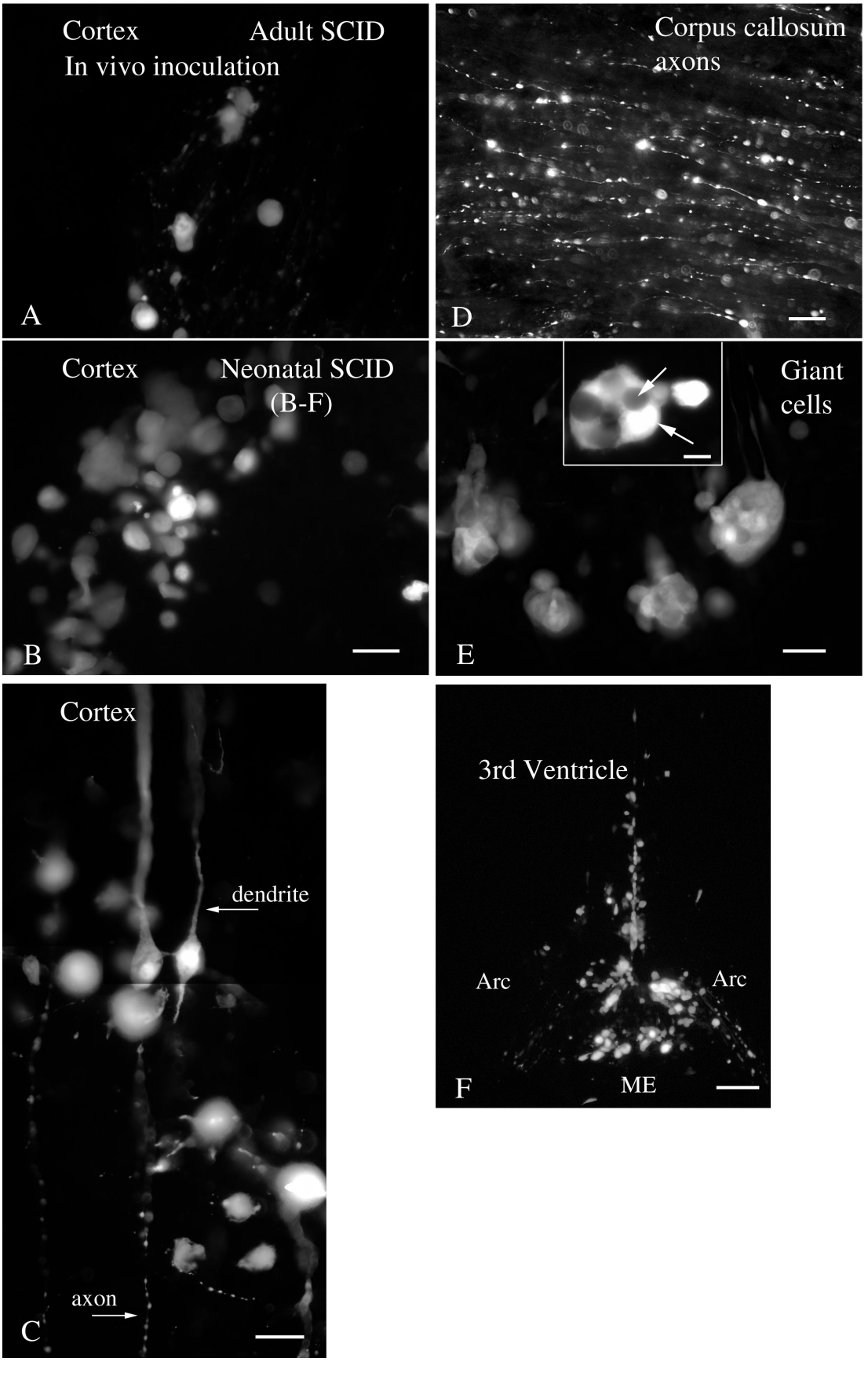
Cortex
Adult SCID
In vivo inoculation
A
Corpus callosum
axons
D
Cortex
Neonatal SCID
(B-F)
B
Giant
cells
E
Cortex
dendrite
axon
C
3rd Ventricle
Arc
Arc
ME
F

below we did not differentiate between cell types, we did find infection of a number of different cell types. Infected cells in the corpus callosum were glial cells; neuronal cell bodies are absent from this white matter area. Neurons were also infected, as shown by the apical dendritic morphology of infected cortical neurons and the ventral course of the efferent axons (Fig. 2C) and also by the presence of GFP in long cortical axons within the corpus callosum (Fig. 2D). Infections of ependymal cells in the walls of the third and lateral ventricles were common (Fig. 2F), as was infection of the choroid plexus. Some regions showed many giant cells composed of a number of cells fused into a single mass (Fig. 2E), typical of CMV infections in the brain.

To determine relative rates of infection, the number of infected cells, determined by expression of the GFP reporter gene, was counted in the different groups. Every GFP-expressing cell body in a section was counted, and the number of infected cells in the entire brain was calculated based on the average number of infected cells multiplied by the total number of sections. Sections from a total of 41 brains were studied; these were divided among four groups of inoculated mice, including adult control ($n = 10$), adult SCID ($n = 8$), neonatal control ($n = 11$), and neonatal SCID ($n = 12$). Analysis of variance (ANOVA) indicated that a substantial difference was found between groups ($P < 0.001$). No difference was found between control and SCID mice when adults were compared to adults and when neonates were compared to neonates ($P > 0.1$) (Fig. 3A). A substantial difference in the number of infected cells was found when adults were compared to neonatal mice. Because no difference was found between age-matched control and SCID mice, the mean of the two groups was used to determine the ratio of infected cells in neonates compared to adults. Neonatal mice (control plus SCID groups) showed about 10-fold more total infected cells than adults (control plus SCID groups) receiving the same viral dose. ANOVA, together with a Tukey-Kramer multiple comparison test, indicated that each neonatal group had substantially more infected cells than each of the adult groups ($P < 0.01$), independent of the immune status of the mouse (Fig. 3A). Although little mortality was found in the adults, a number of neonates died after viral infection: those that died appeared to show even higher numbers of infected cells than the others, as suggested by postmortem analysis of two of these brains. Most of the brains from mice not perfused with fixative were not suitable for analysis due to the tissue deterioration between death and recovery of the brain. Thus, the real difference between adult and neonate is probably even greater than that reported here based on mice that survived the test period. Together, these data strongly support the hypothesis that the developmental status of the brain plays a highly significant role in CMV infection.

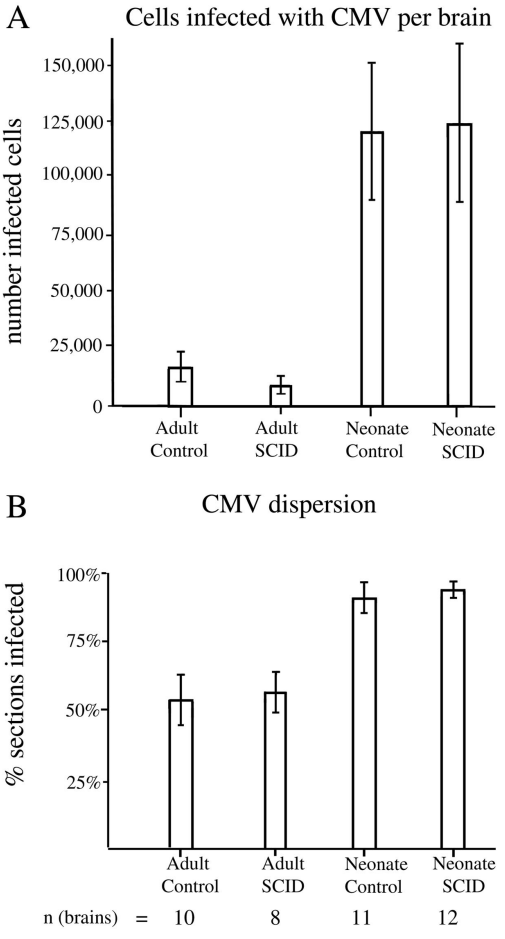

FIG. 3. High level of CMV infection in developing brain- in vivo experiments. (A) CMV-infected cells, identified by GFP expression, were more common in neonatal brains than in adult brains, regardless of immunocompetence. Means ± the SEM are shown. (B) The percentages of histological sections showing CMV infections were compared. SCID and control adult groups had a smaller percentage of infected sections than neonatal SCID and control brains. Means ± the SEM are shown. The total number of brains for each group are shown under each respective bar. A total of 41 brains were evaluated.

In our analysis of the number of brain sections that contained infected cells, we found no difference when adult SCID and adult controls were compared or when neonatal SCID and neonatal control animals were compared. We did find a substantial difference between neonates and adults. A total of 92%

FIG. 2. CMV-infected cells in brain. (A) A small number of cells are infected by CMV in the cortex in the adult SCID mouse. (B) In contrast, a higher number was commonly found in SCID neonatal cortex. (C) Some infected cells show typical morphology of pyramidal neurons, with thick apical dendritic processes and thin axons descending toward the corpus callosum. Note the beaded morphology of the axon, typical of diseased neurons. (D) GFP-labeled axons in the corpus callosum demonstrate that neurons were infected by CMV. (E) Giant cells are commonly found in infected brains, particularly in neonatal mice. Within a single giant cell, labeling was variable, as the two white arrows indicate. (F) Infected cells are common along the ventricular ependymal cells, shown here in the ventral region of the third ventricle and median eminence (ME) in the arcuate nucleus region (Arc) of the hypothalamus. Scale bars: 20 μm in panels A and B; 15 μm in panel C; 10 μm in panel D; 10 μm (inset) and 20 μm in panel E; 50 μm in panel F.

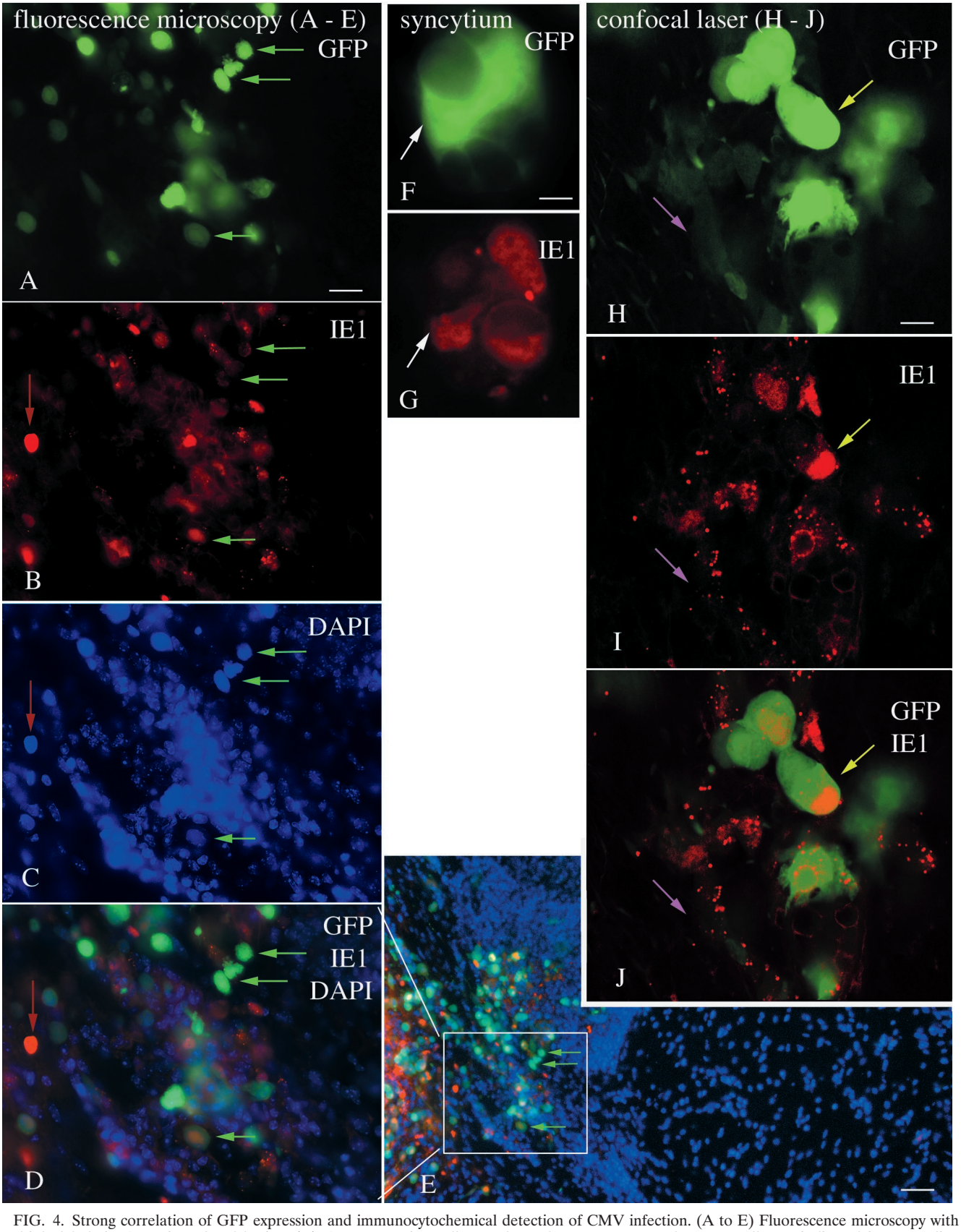

FIG. 4. Strong correlation of GFP expression and immunocytochemical detection of CMV infection. (A to E) Fluorescence microscopy with multiple labels in CMV inoculated brains. (A) GFP-expressing cells are shown by green arrows; the same cells are indicated in succeeding micrographs to facilitate orientation within the section. (B) IE1 immunoreactivity is shown in red. A red arrow indicates a cell that shows little GFP,

of neonatal sections contained infected cells, whereas only 55% of adult sections contained infected cells, a statistically reliable difference (t test; $P < 0.05$) (Fig. 3B). These data indicate a higher degree of spread throughout the CNS in the neonatal brain. This may be due both to a greater degree of viral replication in the neonate and to the smaller size of the neonatal brain.

Comparison of GFP reporter with immunocytochemistry. As a further test for the validity of the use of the GFP reporter, GFP expression was compared with immunocytochemical staining of CMV-infected cells by using an IE1 antiserum detected with the fluorescent label Texas red. IE1 is one of the early proteins synthesized and transported to the nucleus after CMV infects a cell (2, 26, 30). Some brain cells showed both GFP expression in the cytoplasm and red immunolabeling of the nucleus. In addition, other cells showed only red immunolabel or only GFP fluorescence. This would be expected since IE1 protein would be generated first and then would decrease during the time GFP is being synthesized. Anatomically, a high degree of association was found between the two colors. In brain regions with high numbers of GFP-labeled cells, high numbers of red immunoreactive cells were found (Fig. 4A to E). Conversely, regions with no GFP-labeled cells usually had no red immunoreactive cells, as shown in sections triple labeled with GFP, IE1, and the nuclear stain, DAPI (4′,6′-diamidino-2-phenylindole) (Fig. 4E). The number of GFP-expressing cells was compared to the number of red immunolabeled nuclei by using a test square of 400 μm on an edge and placed over 20 different loci of inoculated brains. In inoculated brains, we found a high positive correlation of $r = 0.96$ ($P < 0.01$) between the two indicators of mCMV infection. To achieve a thin optical section in order to facilitate colocalization of GFP and IE1 in the same cells, we used an Olympus confocal scanning microscope. In thin optical sections, most cells that showed red immunoreactivity also showed some GFP expression; some cells showed striking green fluorescence, whereas others showed only a modest green fluorescence (Fig. 4H to J); confocal microscopy showed that infected cells express the GFP reporter gene and had red nuclei containing IE1 immunoreactivity (Fig. 4J). Some cells showing a low level of green fluorescence showed small IE1 immunoreactive red particles, possibly due to IE1 synthesis and transport (Fig. 4H to J). These small particles were not found in control tissue. Giant cells consisting of many fused cells were found in mCMV-infected areas of the brain. These showed GFP fluorescence and Texas red immunolabeling (Fig. 4F and G); in contrast, nearby uninfected cells showed neither green nor red labeling. Based on differential interference contrast imaging and on DAPI staining, we found no giant cells that did not express the GFP reporter. Control brains that were not inoculated showed neither GFP green fluorescence nor red immunolabeling. Control omission of the primary antiserum eliminated specific labeling, as expected. Together, these immunocytochemical data validate the use of the number of GFP-expressing cells as a reliable indicator of relative numbers of mCMV-infected cells in the CNS.

Brain slices infected with CMV. To avoid complications of interpretation due to an intact systemic immune system, we maintained live brain slices from different regions in vitro and infected them with CMV. In all regions of the brain, dramatic differences were evident in the extent of infection among different age groups. Figure 5 shows a photomicrograph of the left half of the brain from a developing mouse and a mature mouse. A typical high degree of infection occurred in the neonate section in vitro, whereas none is found in the slice from the adult brain. Figure 6 shows higher magnification photomicrographs of brain slices at different developmental stages from two regions of the brain, the hippocampus and cerebral cortex, both showing a substantial decrease in infected cells with age. The earliest appearance of GFP expression in younger slices was 5 to 6 h after infection. Infection was minimal at postnatal day 12 (P12) or later in the cortex.

To quantify the perceived variation in infection from one age group to another, we counted the number of cells expressing the reporter gene, GFP, in standard squares of 500 μm on an edge. Thus, brain slices from adult tissue were compared with developing brain tissue from mice of P1, P8, and P12. A total of 31,055 infected cells were counted in inoculated brain slices. In each of the brain regions examined after in vitro infection, including cortex, hippocampus, cerebellum, hypothalamus, and striatum, we found a substantially greater degree of infection in the slices taken from developing brains compared with those taken from mature brains (Fig. 7). The high level of infection in all of these areas is consistent with previous suggestions that the cerebral cortex of the developing mouse brain is particularly susceptible to CMV infection (38, 43). The CA fields and dentate areas of the hippocampus are composed of both glia and neurons. The corpus callosum and the periphery of the hippocampus include primarily glial cells. In each of the eight brain regions studied, the decline in infectivity was consistent and statistically reliable as determined by ANOVA ($P < 0.01$). The decrease in the number of infected cells was not linear. A much greater decrease (70% decrease) was found between P1 and P8 than at any other interval. When all regions of the brain were combined, the level of infection in the adult brain was 4% of that found in the neonates; if the data from the ventricular ependymal cell infections were not included in this analysis, the mean number of infected cells in the adult was 1% of that found in the P1 brain ($P < 0.0001$). This substantial reduction in infectivity to 1% in

but strong immunostaining. The same cell is indicated in panels C and D. (C) The same field as in panels A and B reveals that many cells show no signs of infection; DAPI labels all cells blue. (D) All three colors show the relative number of cells labeled with each color. (E) A low-magnification image of the same region as panel D shows that GFP and red immunofluorescence are found in the same area, whereas to the right a large field of blue cells shows little CMV infection. (F and G) A giant cell, or syncytium of cells, expresses GFP (F) and shows red immunofluorescence (G). (H to J) Confocal scanning laser microscope images of a 1-μm optical section through an infected brain region. (H) Some cells show strong GFP expression (light green arrow), and others show relatively weak expression (pink arrow). The same regions are shown in succeeding micrographs. (I) Red immunofluorescence is strongest in the nucleus, with some granules also showing red fluorescence. (J) A strong overlap of IE1 immunostaining and GFP expression is shown here. Scale bars: 20 μm in panels A to D; 40 μm in panel E; 5 μm in panels F and G; 5 μm in panels H to J.

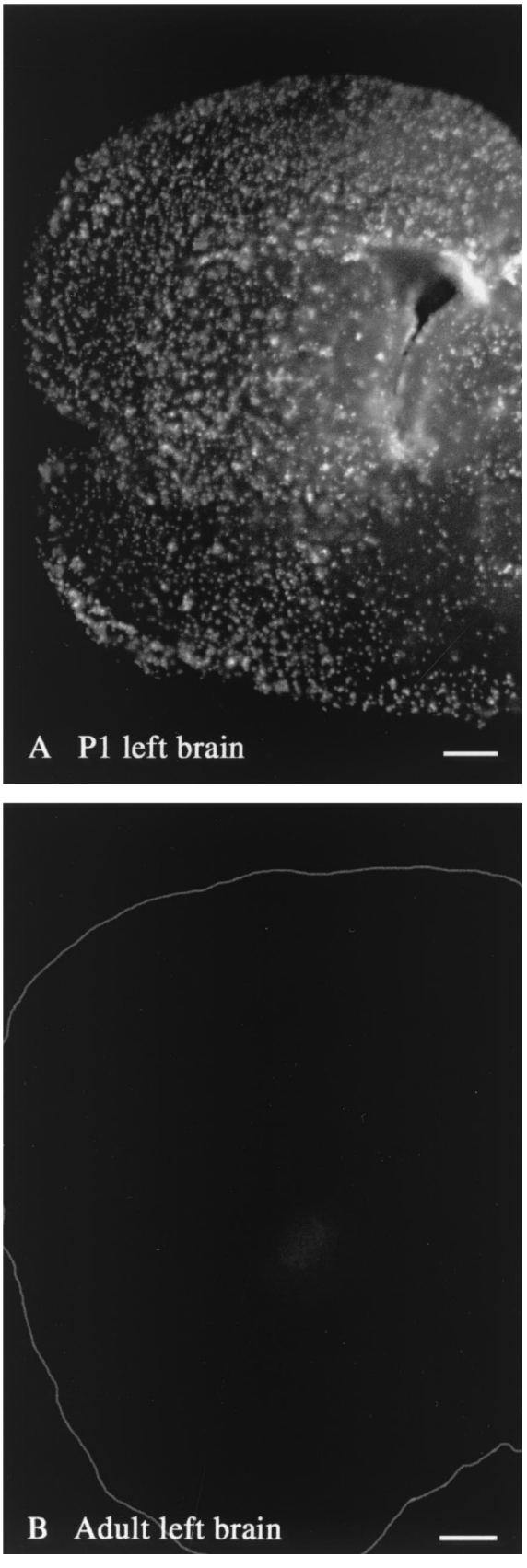

FIG. 5. In vitro CMV infection of left brain in neonate and adult. (A) CMV-infected cells in an in vitro slice from the left side of a P1 brain are abundant in all areas, including cortex, striatum, septum, and preoptic area. (B) In contrast, a corresponding slice from an adult brain shows almost no CMV-infected cells. The perimeter of the adult section is outlined in white. Scale bars: 350 μm in panel A; 800 μm in panel B.

adult slices was found in 7 of the 8 brain regions studied, including regions composed of both neurons and glia (cortex, striatum, hypothalamus, CA1/CA3, and dentate hippocampal fields) and those made up primarily of glia (corpus callosum and hippocampus periphery); the only exception to this dramatic reduction was the ventricular ependyma that continued to show a relatively high level of infection in adults. Embryonic day 16 brain slices showed an even greater degree of infection than any of the postnatal ages (not shown). Because not all of the different brain regions (e.g., hippocampal dentate gyrus) have developed sufficiently at this stage to allow segregation into loci, quantitative data were not included for this age.

One factor that could explain the difference in levels of infection between immature and mature brain slices is that cells in the adult slices died in vitro before they were infected. To control for this possibility, we used a calcium indicator dye, fluo-3, to study calcium responses that would only be found in live cells. At 8 h after preparation of the slices, adult cortical slices were loaded with fluo-3-acetoxymethyl ester for 25 min. The acetoxymethyl ester of fluo-3 becomes fluorescent after being de-esterified inside cells. The fact that cells showed fluo-3-derived fluorescence is an indicator that the plasma membrane was still intact and that endogenous esterases, required to cleave the AM-ester of fluo-3, were still present and active. More important, many cells from the adult cortex showed a calcium increase, seen as an increase in the intensity of fluo-3 fluorescence, in response to stimulation with a micropipette (Fig. 6H and I). These data then support the conclusion that at the time point when cells from younger brain slices are already expressing the GFP reporter gene, adult neurons that show no indication of CMV infection are still alive and do respond to physiological stimuli.

To affirm that CMV was replicating in postnatal day 1 brain slices that showed GFP expression, slices were incubated in BrdU, which is incorporated into newly synthesized DNA, and then immunostained for BrdU. Consistent with previous in vitro studies in other cell types (32), at 48 h after CMV inoculation punctate BrdU labeling was found in brain cells that also showed GFP reporter gene expression. As shown in Fig. 8, GFP expression colocalized to a cytomegalic cell, showing punctate red BrdU labeling; adjacent cells with no GFP showed no BrdU punctate labeling. This punctate labeling is consistent with the view that CMV is replication competent in developing brain slices. Diffuse nuclear labeling with BrdU was found in some cells in both noninfected control and CMV-infected tissue and was suggestive of cell division rather than viral replication.

The primary comparison in these in vitro brain slice experiments was between normal developing and adult brain slices. Since control brain slices showed relatively little CMV infection, we also examined sections from adult SCID mice ($n = 2$ mice; 14 slices). Adult SCID slices showed the same relative absence of CMV infections as the control adults (not shown).

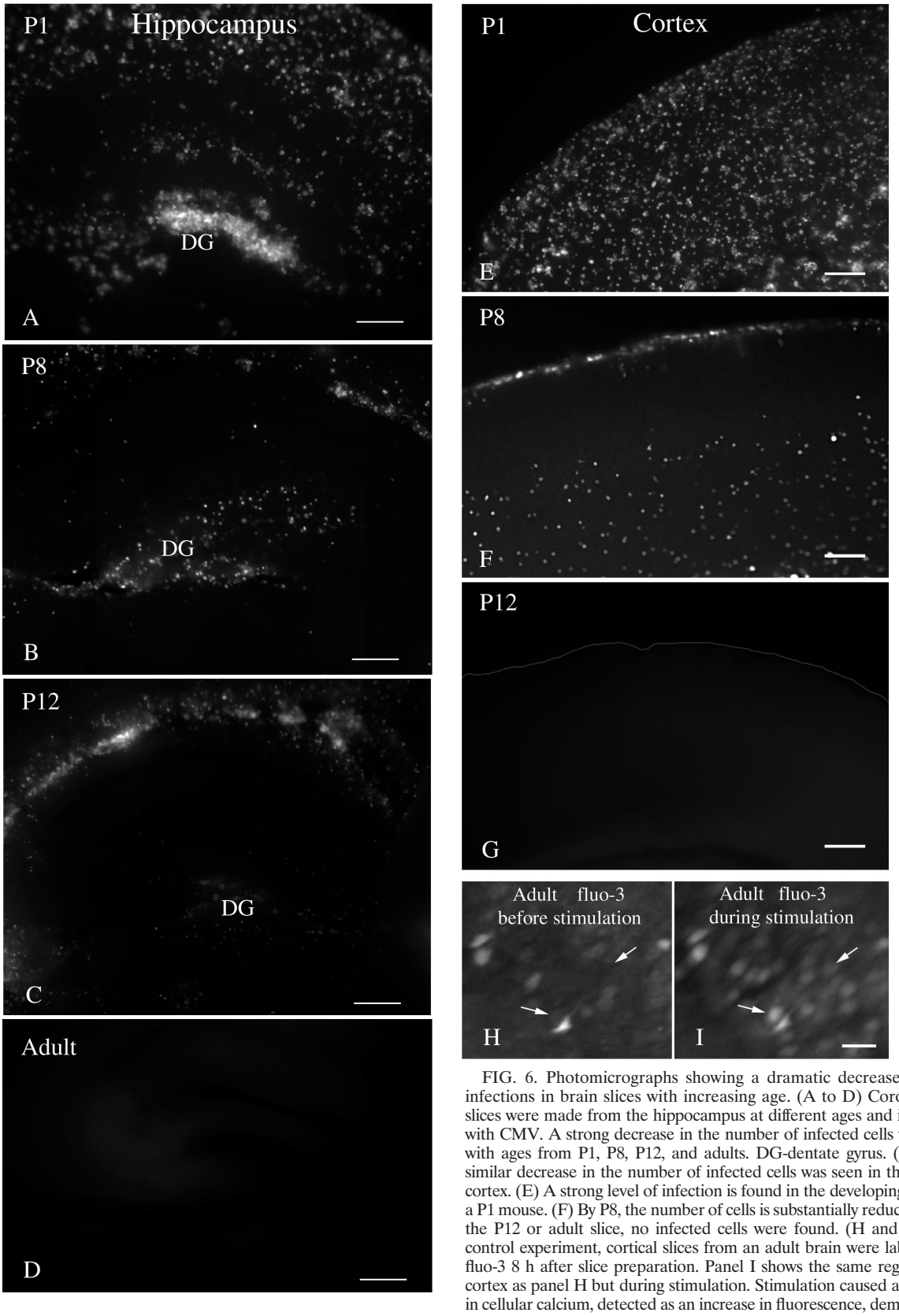

FIG. 6. Photomicrographs showing a dramatic decrease in CMV infections in brain slices with increasing age. (A to D) Coronal brain slices were made from the hippocampus at different ages and inoculated with CMV. A strong decrease in the number of infected cells was found with ages from P1, P8, P12, and adults. DG-dentate gyrus. (E to I) A similar decrease in the number of infected cells was seen in the cerebral cortex. (E) A strong level of infection is found in the developing cortex of a P1 mouse. (F) By P8, the number of cells is substantially reduced. (G) In the P12 or adult slice, no infected cells were found. (H and I) In this control experiment, cortical slices from an adult brain were labeled with fluo-3 8 h after slice preparation. Panel I shows the same region of the cortex as panel H but during stimulation. Stimulation caused an increase in cellular calcium, detected as an increase in fluorescence, demonstrating that the cells were alive. Two of many responding cells are shown by the small arrows in control (H) and stimulated (I) conditions. Scale bars: 200 μm in panel A; 150 μm in panel B; 250 μm in panel C; 250 μm in panel D; 120 μm in panels E, F, and G; 30 μm in panels H and I.

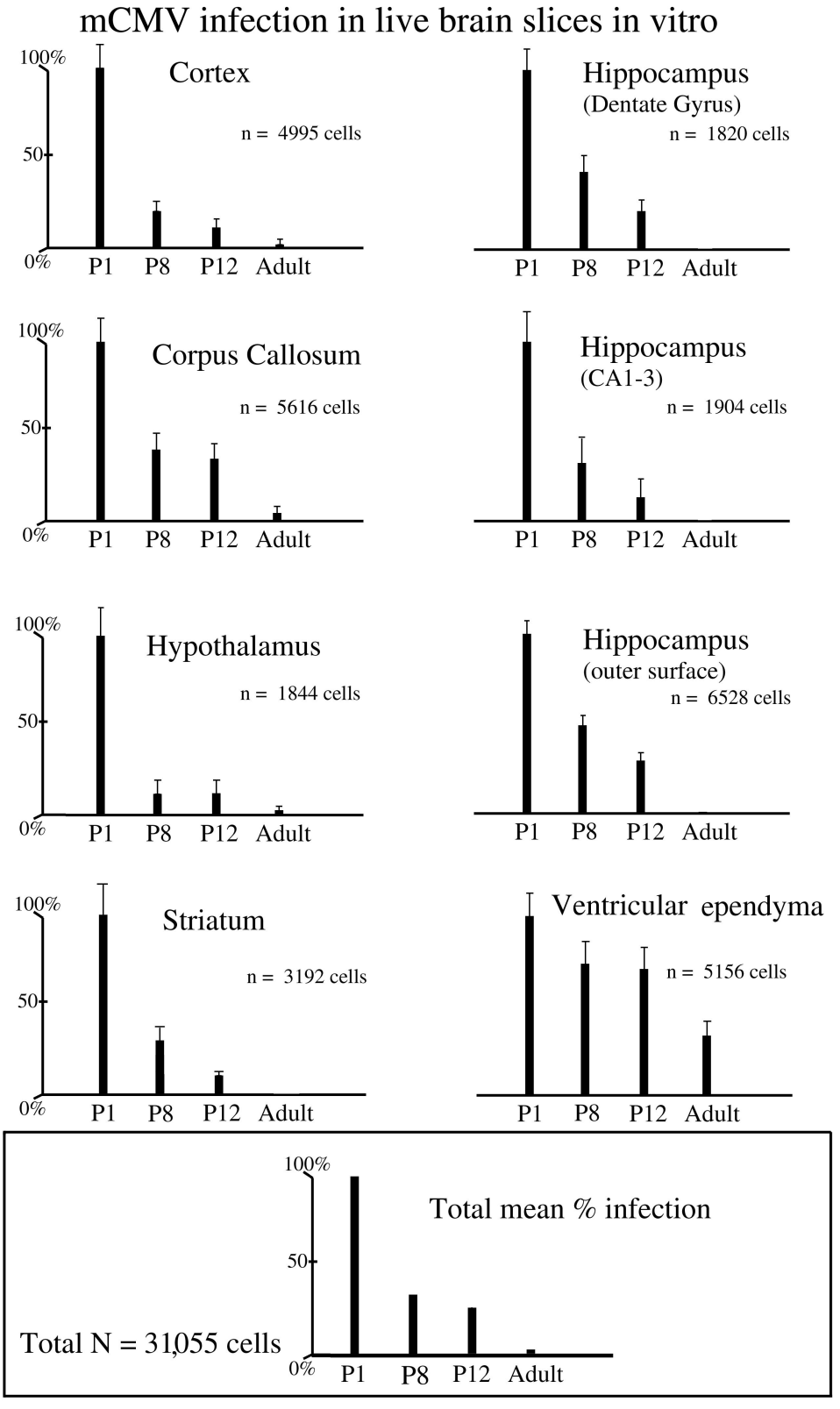

FIG. 7. CMV infection of live brain slice in vitro. A series of eight sets of bar graphs is shown, indicating the relative number of infected cells found at each of 4 brain slice donor ages, for eight different brain regions. The number of infected cells at P1 was standardized as 100%, and the relative number of infected cells found in slices of other ages was determined. In each of the brain regions, a substantial decrease in the number of infected cells was found from P1 to adult. The total number of cells counted for each area is shown in the middle right of each bar graph. The bars indicate means ± the standard deviations. The bottom graph shows the relative mean labeling for the four different age groups when all eight brain regions are combined.

During development, the size of the brain increases. Based on the means from measurements of three mouse brains from each age, we found that the P1 brain (measured in coronal slices at the widest part) was 6 mm wide, the P12 brain was 11 mm wide, and the adult brain was 13 mm wide. In thick slices of the brain inoculated in vitro, infection of cell bodies was restricted to the outer surface of the slice. Thus, the area of a coronal section of an adult mouse would be 4.7 times (difference in widths squared) greater than at P1. One factor that might tend to reduce the total number of cells in a given test area is the increase in brain size. However, the adult brain showed a >100-fold decrease in infected cell number. Even if the number of adult infected cells was multiplied by a correction factor of 4.7, the number of infected cells in the developing P1 brain would still be 20-fold greater than that found in the mature brain. We think these are conservative estimates, since many brain regions such as the cortex or hippocampus showed thousands of infected cells in the neonate in a single slice but showed none in the mature slice of the same region.

In most of the brain, neurogenesis is generally completed before birth; in contrast, in the developing cerebellum, granule cell neurons show peak mitosis around P7 or P8 (36). This gave us the unique opportunity to study CMV infections in brain slices containing large numbers of dividing neurons. Although striking infection of P8 cerebellar slices was found in a layer of cells in the cerebellar cortex, on close examination with differential interference contrast, together with fluorescence microscopy, we found that the infected cells were not the small dividing granule cells but rather were large cells in the Purkinje cell layer (Fig. 9) that completed mitosis embryonically (14, 17). In contrast, control inoculations with a different virus, vesicular stomatitis virus, did selectively infect the dividing granule cells of P8 cerebellar slices (45), indicating that the granule cells were viable and accessible to viral infection. Furthermore, in dispersed neuron cultures, CMV does infect cerebellar granule cells (42), indicating that the selective infection of the Purkinje cell layer is due to a relative affinity for large postmitotic cells rather than an inability to infect granule cells. Adult cerebellum showed little CMV infection (Fig. 9C), indicating a viral preference for immature postmitotic cells. These data suggest that although cell division may be a factor in CMV infections, within the cerebellum infection was found selectively in a region containing the large postmitotic cells of the Purkinje cell layer. This was a consistent finding, as seen from the low magnification micrograph in Fig. 9A.

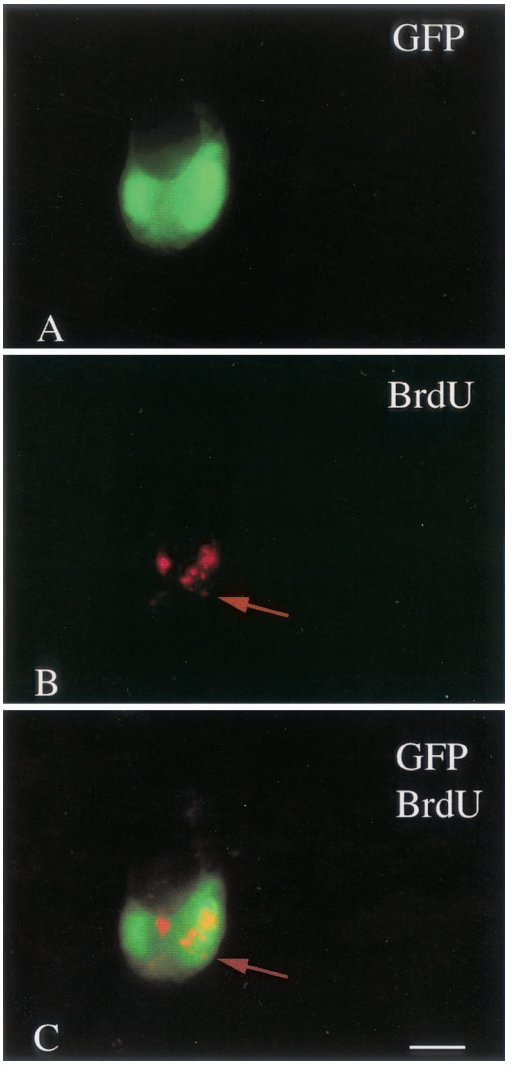

FIG. 8. BrdU incorporation into replicating CMV. (A) A large cell in late stages of infection shows GFP expression. (B) The same cell shows punctate red immunolabeling with Texas red for BrdU, suggesting DNA replication. (C) Colocalization is shown by the overlap of the green GFP expression, together with the red BrdU immunolabeling. Scale bar: 20 μm.

DISCUSSION

The present set of experiments demonstrates that CMV shows a higher level of infection in the developing brain than in the mature brain, regardless of the immune competence of the host. Corroborating experiments show a substantial difference in CMV infections in living brain slices inoculated in vitro, with single neonatal slices showing thousands of infected cells and adult brain slices showing few or none.

These data provide support for the view that CMV has an intrinsic preference for developing brain cells. These data do not argue against the additional importance of the immune system in decreasing CMV infections in mature subjects but rather indicate that factors independent of the adaptive immune system also play a substantial role in the developing brain. These factors may include viral attachment to plasma membrane surface molecules and transport into developing cells, enhanced viral replication, and synthesis of viral proteins. A further deterrent to CMV infections in more mature brains is the physical barrier of the glial sequestering of neurons: sheets of astrocyte membrane often separate one cell from another in the adult brain, reducing the ability of viral particles to gain access to many cells. This glial compartmentalization is lacking in the P1 brain and gradually increases with development (34). Another factor that may reduce CMV infections in mature brain cells is a higher level of endogenous antiviral cytokines and interferons in the mature animal, which may play a role in cellular protection against viruses in the brain (6, 13). CMV is not alone in its predilection for immature neurons; other viruses have also been reported to show an affinity for

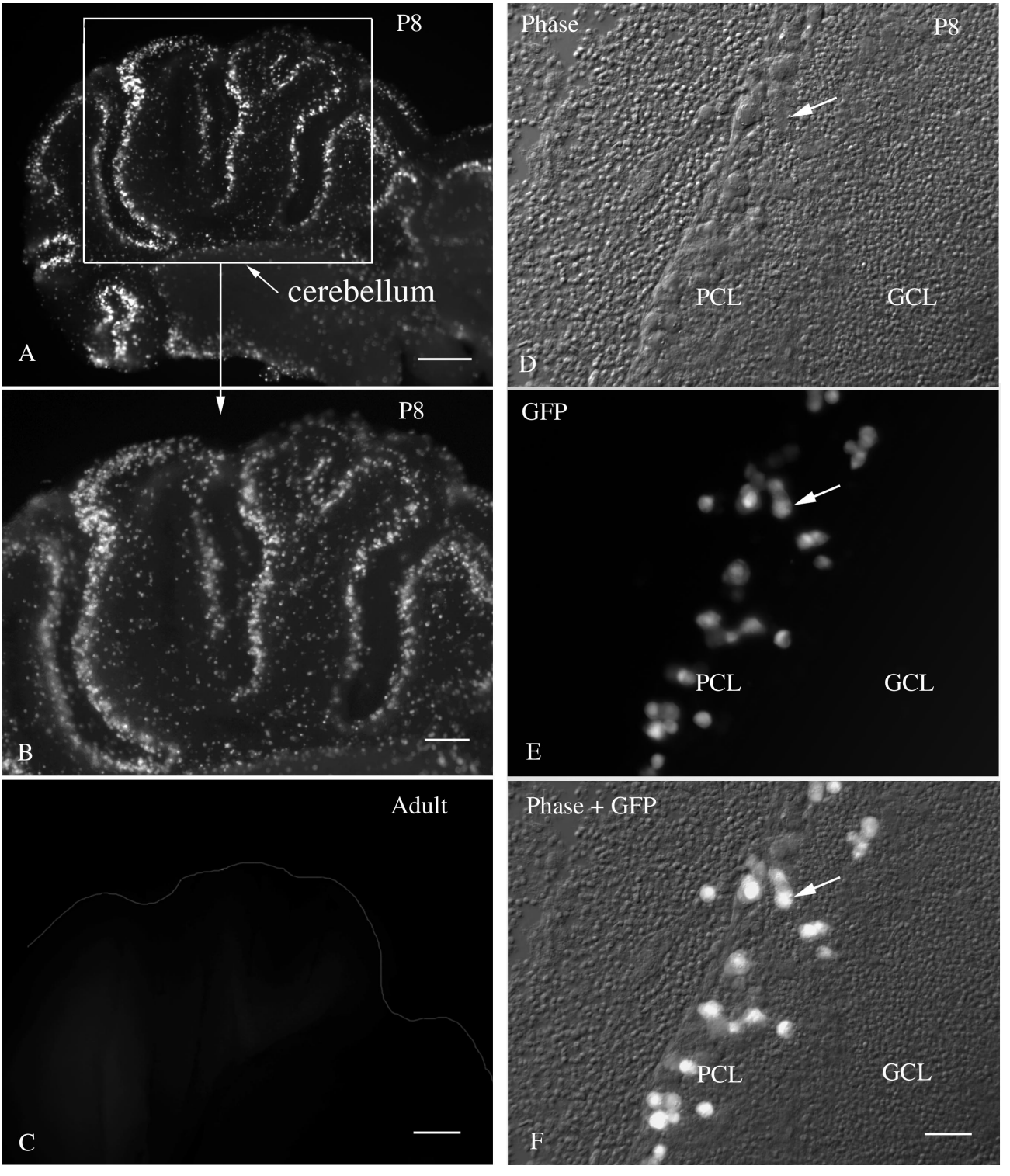

FIG. 9. CMV infection in the P8 cerebellum in vitro. (A and B) Sagittal cerebellar postnatal day 8 slices showed high levels of CMV infection in a band at the periphery of the cerebellar cortex lobules. (C) No indication of infection was found in the cerebellar slice of an adult brain. (D) In this phase-contrast micrograph, the Purkinje cell layer (PCL) and the granule cell layer (GCL) are shown. The arrow indicates a single cell found in panels D to F. (E) Large infected cells showing bright fluorescence are found selectively in the PCL and not in the GCL. (F) Fluorescent and phase images are superimposed to facilitate detection of the infected cells in a background of noninfected cells. Scale bars: 400 μm; in panel A; 200 μm in panel B; 200 μm in panel C; 30 μm in panels D, E, and F.

developing brain cells based on mechanisms not well understood (17a). In the present study with both in vivo and in vitro CNS inoculations, we found that many different cell types were infected by CMV, including neurons, glia, ependymal cells, and cells of the choroid plexus. This is parallel to our work showing that after peripheral CMV inoculation of immunocompromised mice, these same cell types become infected within the CNS (J. D. Reuter, D. L. Gomez, and A. N. van den Pol, Abstr. 101st Gen. Meet. Am. Soc. Microbiol. 2001, abstr. S-7, p. 261, 2001). Although in the present study many cell types were infected, substantial differences existed in the relative probability of infection, particularly in the mature brain where nonneuronal cells, noticeably ependymal cells lining the ventricles, were highly susceptible to infection, whereas mature neurons were resistant, as previously noted in the lateral ventricle (43). The infection of lateral ventricular regions in later development may have ramifications for neuronal replication; one of the few areas of the adult brain where neurons are generated is in the subventricular zone, from which neuronal precursors migrate in the rostral migratory stream to replenish neurons of the olfactory bulb (27, 28). In previous experiments we showed that inoculation of adult human brain slices with mouse CMV resulted in the strongest CMV reporter gene expression in ventricular ependymal cells, although mouse CMV did not appear to replicate in human tissue (43). Thus, the high level of infection in mature mouse ependymal cells in the present study may also be partly independent of replication. Infection of the ventricular wall is a common occurrence in the human brain infected with human CMV (3, 21).

CMV may show an affinity for actively dividing cells (40). However, it is unlikely that this is the sole explanation for our results: in most regions of the brain, neuronal mitosis is completed by P1 (36), the youngest age used in the present work. Glial cell division continues in the neonatal period, and infection of replicating glia may account for some of the infected cells; we previously noted a higher rate of infection and viral replication in cultured astrocytes compared to neurons (42). However, the observation in the present study that the CMV infection was stronger in some nondividing cells than in cells undergoing mitosis in the same region argues against mitosis as being the sole determining factor here. For instance, in the cerebellum, we found relatively little infection of the external granule cells that undergo a relatively late round of cell division at P8 (the developmental age used here), whereas postmitotic cells in the same brain slice in the Purkinje cell layer showed robust CMV infection. Rhabdoviruses used in parallel experiments showed a preferential affinity for the dividing granule neurons in sister cerebellar tissue slices of the same developmental stage (45), indicating a selective affinity of CMV for the large cells of the Purkinje cell layer.

The high rate of infection in developing brains parallels the high expression of reporter genes under control of the CMV IE1 promoter in transgenic mice. IE1 promoter-regulated reporter gene expression was greater in developing brains than in mature transgenic brains (24, 25, 46). The higher rate of IE1 promoter expression in developing brain suggests that another mechanism favoring CMV infection in developing brain could be a higher level of activation of the IE1 promoter, leading to greater levels of IE1 protein generation that may enhance infection levels.

In the present study we found no statistical difference in infection rates between control and SCID mice. This lack of difference is most likely due to the short postinoculation experimental duration of less than a week, a period dictated by the high neonatal mortality rate during a longer postinoculation interval. Compared to normal controls, a substantially greater degree of CMV infection is found in the peripheral organs and retinas of SCID mice when they were maintained for a long survival time; SCID mice also show a higher degree of mortality from CMV infections (1, 15, 29, 35). After peripheral CMV infection, we find no difference in CNS infection between SCID and controls after a week, but at longer intervals we find a high degree of infection in SCID, but not control, mouse brains (Reuter et al., Abstr. 101st Gen. Meet. Am. Soc. Microbiol. 2001). Another factor that may play a role here is that the blood-brain barrier that normally acts to restrict infections by viruses may also reduce the ability of cells of the systemic immune system to detect and control CMV infections once established within the brain.

In conclusion, data from our work with intracranial injections in neonatal and adult control and SCID mice show that, independent of the adaptive immune system (T and B cells), CMV infections are substantially greater in the developing brain. With our converging use of live brain slices inoculated in vitro, we further show that developing brain tissue from hypothalamus, cortex, hippocampus, striatum, and cerebellum is more susceptible to CMV infection independent of the whole systemic immune system (T and B lymphocytes, natural killer cells, and macrophages/monocytes). The greater level of infection of developing brain may be due to a combination of viral affinity for developing brain cells and to the absence of intrinsic cellular mechanisms to combat viral infections within the developing brain.

ACKNOWLEDGMENTS

We thank Y. Yang and S. Hill for excellent technical facilitation in these studies, M. Carrithers for helpful comments on the manuscript, and E. Markakis for suggestions on BrdU labeling.

This work was supported by NIH grants NS37788, NS34887, and AI/NS48854.

REFERENCES

1. **Abenes, G., M. Lee, E. Haghjoo, T. Tong, X. Zhan, and F. Liu.** 2001. Murine cytomegalovirus open reading frame M27 plays an important role in growth and virulence in mice. J. Virol. **75:**1697–1707.
2. **Ahn, J. H., and G. S. Hayward.** 1997. The major immediate-early proteins IE1 and IE2 of human cytomegalovirus colocalize with and disrupt PML-associated nuclear bodies at very early times in infected permissive cells. J. Virol. **71:**4599–4613.
3. **Alford, C. A., and W. J. Britt.** 1996. Cytomegalovirus, p. 2493–2534. *In* B. N. Fields, D. M. Knipe, and P. M. Howley (ed.), Fields virology, 3rd ed. Lippincott-Raven Publishers, New York, N.Y.
4. **Bale, J. F., Jr, P. F. Bray, and W. E. Bell.** 1985. Neuroradiographic abnormalities in congenital cytomegalovirus infection. Pediatr. Neurol. **1:**42–47.
5. **Booss, J., P. R. Dann, B. P. Griffith, and J. H. Kim.** 1989. Host defense response to cytomegalovirus in the central nervous system. Am. J. Pathol. **134:**71–78.
6. **Bowden, R. A., S. Dobbs, D. Amos, and J. D. Meyers.** 1990. Comparison of interleukin-2 and gamma-interferon production by peripheral blood mononuclear cells in response to cytomegalovirus after marrow transplantation. Transplantation **50:**38–42.
7. **Britt, W. J., and L. G. Vugler.** 1990. Antiviral antibody responses in mothers and their newborn infants with clinical and subclinical congenital cytomegalovirus infections. J. Infect. Dis. **161**:214–219.
8. **Brutkiewicz, R. R., and R. M. Welsh.** 1995. Major histocompatibility complex class I antigens and the control of viral infections by natural killer cells. J. Virol. **69:**3967–3971.

9. **Brutkiewicz, R. R., J. R. Bennink, J. W. Yewdell, and A. Bendelac.** 1995. TAP-independent, β_2-microglobulin-dependent surface expression of functional mouse CD1.1. J. Exp. Med. **182:**1913–1919.
10. **Bukowski, J. F., B. A. Woda, and R. M. Welsh.** 1984. Pathogenesis of murine cytomegalovirus infection in natural killer cell-depleted mice. J. Virol. **52:** 119–128.
11. **Cardin,R.D., G.B.Abenes, C.A.Stoddart, E. S. Mocarski.** 1995. Murine cytomegalovirus IE2, an activator of gene expression, is dispensible for growth and latency in mice. Virology **209:**246–251.
12. **Charles, A. C.** 1994. Glia-neuron intercellular calcium signaling. Dev. Neurosci. **16:**196–206.
13. **Cheeran, M. C., S. Hu, S. L. Yager, G. Gekker, P. K. Peterson, and J. R. Lokensgard.** 2001. Cytomegalovirus induces cytokine and chemokine production differentially in microglia and astrocytes: antiviral implications. J. Neurovirol. **7:**135–147.
14. **del Cerro, M., and J. R. Swarz.** 1976. Prenatal development of Bergmann glial fibres in rodent cerebellum. J. Neurocytol. **5:**669–676.
15. **Duan, J., W. Paris, P. Kibler, C. Bousquet, M. Liuzzi, and M. G. Cordingley.** 1998. Dose and duration-dependence of ganciclovir treatment against murine cytomegalovirus infection in severe combined immunodeficient mice. Antiviral Res. **39:**189–197.
16. **Giblett, E. R., A. J. Ammann, D. W. Wara, R. Sandman, and L. K. Diamond.** 1975. Nucleoside-phosphorylase deficiency in a child with severely defective T-cell immunity and normal B-cell immunity. Lancet **7914:**1010–1013.
17. **Goffinet, A. M.** 1983. The embryonic development of the cerebellum in normal and reeler mutant mice. Anat. Embryol. **168:**73–86.

17a. **Griffin, D. E., and J. M. Hardwick.** 1999. Perspective: virus infections and the death of neurons. Trends Microbiol. **7:**155–160.

18. **Grundy, J. E., J. S. Mackenzie, and N. F. Stanley.** 1981. Influence of *H-2* and non-*H-2* genes on resistance to murine cytomegalovirus infection. Infect. Immun. **32:**277–286.
19. **Hendrikson, E. A., D. G. Schatz, and D. T. Weaver.** 1988. The *scid* gene encodes a trans-acting factor that mediates the rejoining event of Ig gene arrangement. Genes Dev. **2:**817–829.
20. **Hicks, T., K. Fowler, M. Richardson, A. Dahle, L. Adams, and R. Pass.** 1993. Congenital cytomegalovirus infection and neonatal auditory screening. J. Pediatr. **123:**779–782.
21. **Ho, M.** 1991. Cytomegalovirus: biology, and infection: current topics in infectious disease. Plenum Medical Books, New York, N.Y.
22. **Ho, K. L., C. Gottlieb, and R. J. Zarbo.** 1991. Cytomegalovirus infection of cerebral astrocytoma in an AIDS patient. Clin. Neuropathol. **10**:127–133.
23. **Johnson, R. T.** 1998. Viral infections of the nervous system. Lippincott-Raven Publishers, New York, N.Y.
24. **Koedood, M., A. Fichtel, P. Meier, and P. J. Mitchell.** 1995. Human cytomegalovirus (CMV) immediate-early enhancer/promoter specificity during embryogenesis defines target tissue of congenital HCMV infection. J. Virol. **69:**2194–2207.
25. **Kothary, R., S. C. Barton, T. Franz, M. L. Norris, S. Hettle, and M. A. Surani.** 1991. Unusual cell specific expression of major human cytomegalovirus immediate early gene promoter-*lazZ* hybrid gene in transgenic mouse embryos. Mech. Dev. **35:**25–31.
26. **LaFemina, R. L., M. C. Pizzorno, J. D. Mosca, and G. S. Hayward.** 1989. Expression of the acidic nuclear immediate-early protein (IE1) of human cytomegalovirus in stable cell lines and its preferential association with metaphase chromosomes. Virology **172:**584–600.
27. **Lois, C., J. M. Garcia-Verdugo, and A. Alvarez-Buylla.** 1996. Chain migration of neuronal precursors. Science **271:**978–981.
28. **Luskin, M. B.** 1998. Neuroblasts of the postnatal mammalian forebrain: their phenotype and fate. J. Neurobiol. **36:**221–233.
29. **Mizota, A., D. I. Hamasaki, and S. S. Atherton.** 1991. Physiologic and morphologic retinal changes induced by murine cytomegalovirus in BALB/c and severe combined immune deficient mice. Investig. Ophthalmol. Vis. Sci. **32:**1479–1491.
30. **Mocarski, E.** 1996. Cytomegaloviruses and their replication, p. 2447–2492. *In* B. N. Fields, D. M. Knipe, and P. M. Howley (ed.), Fields virology, 3rd ed. Lippincott-Raven Publishers, New York, N.Y.
31. **Osborn, J. E.** 1982. Cytomegalovirus and other herpesviruses, p. 267–292. *In* H. L. Foster, J. D. Small, and J. G. Fox (ed.), The mouse in biomedical research. II. Diseases. Academic Press, New York, N.Y.
32. **Penford, M. E. T., and E. S. Mocarski.** 1997. Formation of cytomegalovirus DNA replication compartments defined by localization of viral proteins and DNA synthesis. Virology **239:**46–61.
33. **Perez-Jiminez, A., V. Colamaria, A. Franco, R. Grimau-Merino, R. Darra, E. Fontana, E. Zullini, A. Beltramello, and B. Dalla-Bernardina.** 1998. Epilepsy and disorders of cortical development in children with congenital cytomegalovirus infection. Rev. Neurol. **26:**42–49.
34. **Peters, A., S. L. Palay, and H. de F. Webster.** 1991. The fine structure of the nervous system: neurons and their supporting cells. Oxford University Press, New York, N.Y.
35. **Reynolds, R. P., R. J. Rahija, D. I. Schenkman, and C. B. Richter.** 1993. Experimental murine cytomegalovirus infection in severe combined immunodeficient mice. Lab. Anim. Sci. **43:**291–295.
36. **Schambra, U. B., J. Lauder, and J. Silver.** 1991. Atlas of the prenatal mouse brain. Academic Press, New York, N.Y.
37. **Selgrade, M. J., and J. E. Osborn.** 1974. Role of macrophages in resistance to murine cytomegalovirus. Infect. Immun. **10:**1383–1390.
38. **Shinmura, Y., I. Kosugi, M. Kaneta, and Y. Tsutsui.** 1999. Migration of virus infected neuronal cells in cerebral slice cultures of developing mouse brains after in vitro infection with murine cytomegalovirus. Acta Neuropathol. **98:**590–596.
39. **Starr, S. E., and A. C. Allison.** 1977. Role of T lymphocytes in recovery from murine cytomegalovirus infection. Infect. Immun. **17:**458–462.
40. **Stinski, M. F.** 1977. Synthesis of proteins and glycoproteins in cells infected with human cytomegalovirus. J. Virol. **23:**751–767.
41. **Tsutsui, Y., A. Kashiwai, N. Kawamura, S. A. Aiba-Masago, and I. Kosugi.** 1995. Prolonged infection of mouse brain neurons with murine cytomegalovirus after pre- and perinatal infection. Acta Virol. **140:**1725–1736.
42. **van den Pol, A. N., E. Mocarski, N. Saederup, J. Vieira, and T. J. Meier.** 1999. Cytomegalovirus cell tropism, replication, and gene transfer in brain. J. Neurosci. **19:**10948–10965.
43. **van den Pol, A. N., J. Vieira, D. D. Spencer, and J. G. Santarelli.** 2000. Mouse cytomegalovirus in developing brain tissue: analysis of 11 species with GFP-expressing recombinant virus J. Comp. Neurol. **427:**559–580.
44. **van den Pol, A. N., X. B. Gao, P. Patrylo, P. Ghosh, and K. Obrietan.** 1998. Glutamate inhibits GABA excitatory activity in developing neurons. J. Neurosci. **18:**10749–10761.
45. **van den Pol, A. N., K. Dalton, and J. Rose.** 2002. Relative neurotropism of a recombinant rhabdovirus expressing a green fluorescent envelope glycoprotein. J. Virol. **76:**1309–1327.
46. **van den Pol, A. N., and P. Ghosh.** 1998. Selective neuronal expression of green fluorescent protein with cytomegalovirus promoter reveals entire neuronal arbor in transgenic mice. J. Neurosci. **18:**10640–10651.
47. **White, D. O., and F. J. Fenner.** 1994. Medical virology. Academic Press, New York, N.Y.